

# Coordination of Multi-digit Positions and Forces During Unconstrained Grasping in Response to Object Perturbations

Abdeldjalil Naceri\*  
Department of Cognitive  
Neuroscience & CITEC,  
Bielefeld University,  
Bielefeld 33615

Alessandro Moscatelli †  
Department of Cognitive  
Neuroscience & CITEC,  
Bielefeld University,  
Bielefeld 33615

Marco Santello ‡  
School of Biological and Health  
Systems Engineering,  
Arizona State University Tempe,  
Arizona 85287

Marc O. Ernst §  
Department of Cognitive  
Neuroscience & CITEC,  
Bielefeld University,  
Bielefeld 33615

## ABSTRACT

When humans grasp and manipulate objects there are many choices to make, such as where to place the digits or how much force each digit should apply. This problem is highly unconstrained as infinitely many different combinations of finger positions and force distributions lead to stable grasps. This is due to the many redundancies at different levels of the sensorimotor system. In this paper, we investigate the strategy used by humans in distributing finger positions and forces while a hand-held object was perturbed by force and torque in a predictable or unpredictable fashion. Our results revealed that there was a substantial systematic variability among participants' initial placement of the digits on the object. However, within participants' digit placement was rather stereotypical. Moreover, the normal forces applied by the digits co-varied with their initial horizontal and vertical placements. Importantly, we recorded an effect of the horizontal and vertical shift between the thumb and the virtual finger positions on the grip force. Principal component analysis revealed that more than 95% of the digit force variance was accounted by the first two components. Finally, participants learned to compensate the external torque within the first perturbations within each trial during the holding phase. We propose that digit forces were modulated online based on self-chosen digit locations during the holding phase in order to successfully compensate sudden external torques.

**Index Terms:** Human-centered computing [Human computer interaction (HCI)]: HCI design and evaluation methods;

## 1 INTRODUCTION

Small children learn to grasp objects before learning to walk or to talk. Grasping and handling objects found in daily life (e.g., cell phones, books, door handles, etc.) is one of the basic ways in which humans interact with their environment. Yet, grasping is a complicated task when considered at the cognitive level. Grasping and manipulating objects accurately is achieved by modulating finger locations and forces using sensory feedback from the fingertips and other modalities such as vision. Moreover, force modulation to object properties can also be implemented in an anticipatory fashion prior to the onset of manipulation [8]. Specifically, it has been shown that participants anticipated the properties of the grasped object (i.e. center of mass in different locations) in terms of where to place the fingers and how much force to apply [6, 9]. The sensorimotor mechanisms underlying anticipatory control of digit positions on the object and the distribution of finger forces for dexterous manipulation are not fully understood. Grasping can be performed

successfully in an infinite number of ways due to the large number of degrees of freedom in the human hand (more than the number required by the task). Successful grasping and manipulation require that the central nervous system master redundancy in degrees of freedom such as digit contact point selection, forces and torques to be applied, and to select an appropriate hand posture [3, 4]. A stable grasp, after successfully selecting the digit locations on the grasped object, is defined by satisfying slip preventions, tilt prevention, and perturbation resistance [19]). Slip prevention is attained by force modulation that satisfies the safety margin, that is, the digits have to apply grasp forces above the required minimum that is necessary to hold the object against gravity [8]. For tilt prevention and to accurately maintain the orientation of the object, digit forces have to be distributed such as to compensate the external torque acting on the object [19]. Resistance to perturbations is defined as the forces that the digits have to produce in order to ensure a stable grasp when mechanical perturbations are present [19]. Recent work on grasping and manipulation, have investigated hand kinematics and the hand postures for tasks that allow choice of digit placement, i.e., unconstrained grasping [4, 14]. In contrast, several studies have focused on multi-digit force synergies (dynamics) using fixed digit contact locations (constrained grasping) due to the fixed locations of force sensors [2, 15, 19]. Yet another pool of studies has focused on sensorimotor learning of manipulation using unconstrained multi-digit grasping tasks without examining digit forces [9]. Fu *et al.* [6] have made the first step into investigating anticipatory control of both digit locations and forces using two-digit (thumb and index finger) grasping by comparing constrained and unconstrained grasping. This study showed that subjects modulate digit forces as a function of digit placement when they can choose contact points [6]. Hence, during unconstrained grasping, the spatial locations of each digit are independent parameters that the sensorimotor system can modulate in order to control the grip force [6]. In this work, we aim to provide insight into the modulation of multi-digit forces for a whole-hand unconstrained grasping task. To this end, a tactile force sensing device of rectangular cuboid shape was designed to measure the spatial location of each digit using its Cartesian coordinates (x,y) rather than focusing only one coordinate (i.e., vertical placement on the object) as done previously [6, 9]). Finally, previous studies have used the approach of changing location of the objects center of mass to generate external torques to quantify subjects' ability to learn a compensatory torque at object lift onset [6, 5, 9]. Thereby, participants experienced the perturbation at the lift onset, i.e., while the hand was moving. For our study, we designed an experimental setup and developed a protocol in order to generate force and torque perturbations while subjects hold the object statistically and generate steady state forces and torques. We used force perturbations to evaluate the stability of the grasp and investigate changes in the force distribution across the digits during the application of either predictable (periodic) or unpredictable (aperiodic) force perturbations. The goal of our experimental approach was to evaluate how subjects learned to resist the perturbations by modulating digit normal forces and their locations in response to mechanical perturbations.

\*e-mail:abdeldjalil.naceri@uni-bielefeld.de

†e-mail:alessandro.moscatelli@uni-bielefeld.de

‡e-mail:marco.santello@asu.edu

§e-mail:marc.ernst@uni-bielefeld.de

## 2 METHODS

### 2.1 Participants

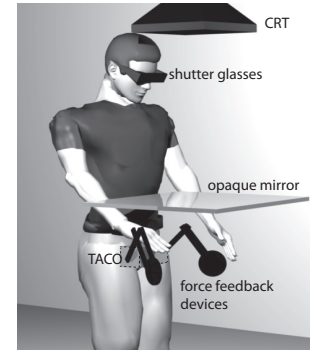
Seven right-handed participants,  $29 \pm 4$  years of age (4 males), took part for the first time in the experiment. All participants were without neurological or motor deficit and they gave informed written consent in accordance with the Declaration of Helsinki.

### 2.2 Hardware

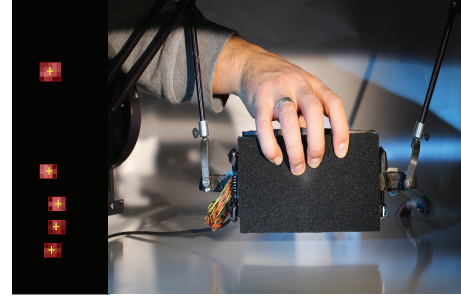
For our study, we built a Tactile Object (TACO) that is able to record the position and normal force exerted by each finger on the object, while allowing participants to choose digit placement and to grasp the object in an unconstrained fashion. The TACO is of rectangular cuboid shape (length:  $l = 170$  mm, height:  $h = 85$  mm and width  $w = 55$  mm) and it is constructed using four modules of high-speed tactile sensor (up to 1.9 kHz) developed by Schurmann *et al.* [16]. Each module of size  $80 \times 80$  mm<sup>2</sup> provides a matrix of  $16 \times 16$  of tactels with 5 mm of spatial resolution. Thus, the output matrix of TACO is  $64 \times 16$  tactels, while two of the modules are mounted on the front side of TACO and two on its back. Thus, TACO allows us to simultaneously record the position of all five fingers of the grasping hand, including the normal forces exerted by the fingers. TACO is calibrated using a force gauge with a force ranging from 0 to 25 N and we varied also gauge tip across sections from 10 to 50 mm<sup>2</sup> with a step of 20 mm<sup>2</sup>. Participants viewed a virtual rectangular cuboid while they grasped the TACO and they had no visual feedback of their actual hand location in the scene. The visual scene was displayed on a 21 CRT-computer monitor (SONY® CPD-G520) with a resolution of  $1280 \times 1024$  pixels (refresh rate 100 Hz). Participants viewed the mirror image of the visual scene via liquid-crystal shutter glasses (CrystalEyes™) providing binocular disparity (Figure 1a). The TACO was attached to two PHANToM™ (SensAble® Technologies) forces feedback devices in order to track its position and to apply force/torques perturbations while participants held the TACO in one hand (Figure 1b). The sampling rate of the PHANToM™ was 1 kHz. The total weight of TACO attached to the PHANToM™ arms was  $m = 0.470$  kg. Constrained by the arrangement of the PHANToM™ force feedback devices, TACO has five degrees of freedom of unconstrained motion ( $x, y, z, 0$ : no pitch rotation,  $\alpha$ : yaw,  $\beta$ : roll).

### 2.3 Procedure

Participants sat on a chair of adjustable height. Before the start of the grasping movement participants forearm rested on a plank with the palm of the hand facing downward. Participants received an auditory "GO" signal instructing them to start the grasp and lift the TACO 100 to 150 mm. To indicate the appropriate height for stabilizing the TACO, the virtual rectangular cuboid color changed when they reached the desired height. At that height, participants were asked to hold the TACO as still as possible for 20 s irrespective of any disturbance forces acting on the object. The finger locations on the TACO were self-chosen (grasping without constraints). After having stabilized the TACO for approximately 20 s, participants received another auditory signal cueing them to replace the TACO on the table. During the object hold phase, perturbation forces and torques were applied using the PHANToM™ force feedback devices. We studied 3 conditions of force/torque perturbations: force of  $F_y = 2.4$  N (Figure 2a) was applied in vertical direction, torques with a total amount of 0.25 N·m were applied around the y- and z-axis (Figures 2b, 2c respectively) causing yaw and roll rotations around TACO's center of mass. The applied force and torques ( $F_y$ ,  $T_y$  and  $T_z$ ) were turned "on" and "off" periodically (perturbation frequency) in one condition and were thus "predictable" in terms of frequency (Figure 2d). In the other condition, the applied force and torques were turned on aperiodically (i.e. perturbations "on" ranged in length between 1 to 3.5 msec and perturbations "off" ranged in length between 0.6 to 1 sec; both randomly presented)



(a) Setup



(b) Tactile Object (TACO) with its output image

Figure 1: Experimental materials. (a) Participants binocularly view the mirror image of the visual scene. (b) The TACO attached to the PHANToM™ force feedback devices. On the left, the TACO output image with yellow cross represents digit center of pressures ( $CoPs$ ).

and were thus "unpredictable" (Figure 2e). The rationale of this experimental design was to test whether the grasping forces of the fingers would adapt to the different temporal patterns depending on whether or not the perturbations were predictable or not. Both perturbation torques ( $T_z$  and  $T_y$ ) were applied in clock-wise (CW) and counter-clock-wise (CCW) directions. Thus, there were in total 10 conditions: ( $F_y$ ,  $T_y^{CCW}$ ,  $T_y^{CW}$ ,  $T_z^{CCW}$ ,  $T_z^{CW}$ ) with both periodic and aperiodic (P/Ap). The order of conditions was randomly presented to the participants. Ten trials were conducted for each condition. Each trial lasted approximately 25 s from grasp onset to the end. Before starting the experiments, subjects performed four trials with  $F_y$  perturbation in order to familiarize with the task. Participants could rest as much as they wanted between two consecutive trials. The total duration of the experiment was approximately two hours per subject with a break of one hour in the half of the experiment.

## 3 DATA PROCESSING AND ANALYSIS

The normal forces  $F$  of the fingers and the center of pressures  $CoP_x$  and  $CoP_y$  were directly read from the force modules of the TACO. The  $CoP_x$  and  $CoP_y$  were defined as the location of the maximally (one output: global maximum of the activated region) activated tactels for each fingers' region in the output matrix that was converted to force in Newton using the lookup table from the calibration. The calibration table was obtained with a resolution  $\pm 0.2$  N. Digit locations, normal forces, and TACO position were recorded and ran through a second order Butterworth low pass filter with 1 Hz cutoff frequency (Figure 3). Digits locations  $CoP_x$  and  $CoP_y$  were both extracted during the holding phase. In addition, the grip force ( $F_{Grip}$ ) was calculated as sum of absolute magnitude of digit normal forces. The  $CoP$  of the virtual finger was calculated as the average of the four fingers'  $CoPs$  opposing the thumb. We denote  $\Delta CoP_x$  and  $\Delta CoP_y$  as the horizontal and vertical

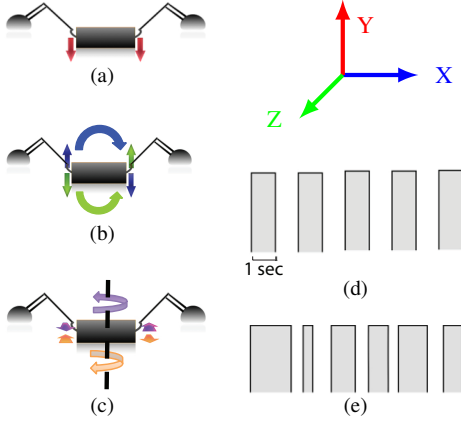


Figure 2: Experimental protocol. (a) Perturbation force  $F_y$ . (b) Perturbation torque  $T_z$  CW and CCW. (c) Perturbation torque  $T_y$  CW and CCW. (d) periodic (e) aperiodic with gray areas represents when force/torque perturbation is on.

distances between the thumb and the virtual finger. The positions and rotations of TACO were tracked using PHANToM<sup>TM</sup> devices. They were used to compute the participants' hand net torques  $HT_{y,z}$  using the Newton's second law for rotation:

$$\begin{cases} HT_y + T_y = \frac{d^2\alpha}{dt^2} I_y \\ HT_z + T_z = \frac{d^2\beta}{dt^2} I_z \end{cases} \quad (1)$$

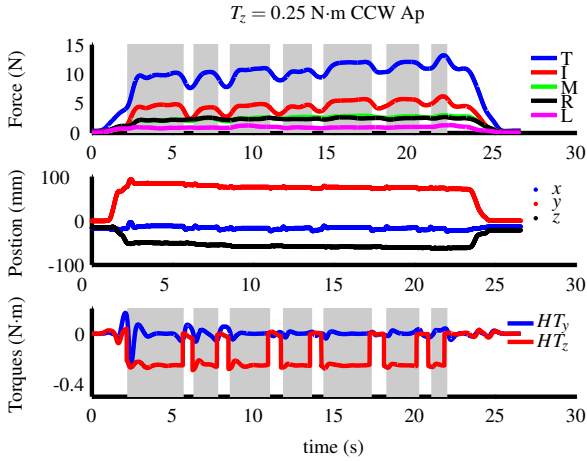


Figure 3: Digit normal forces, TACO position and hand torques for representative subject. Gray areas represents intervals when perturbations "on". Legend 1: T: thumb, I: index, M: middle, R: ring, L: little. Legend 2:  $x, y, z$  are the TACO's coordinates. Legend 3:  $HT_y, HT_z$  are the hand net torque.

where  $T_y, T_z$  are external torques,  $\frac{d^2\alpha}{dt^2}$  and  $\frac{d^2\beta}{dt^2}$  are the angular accelerations, and  $I_y$  and  $I_z$  are approximated to a rectangular cuboid moments of inertia:

$$\begin{cases} I_y = \frac{1}{12}m(l^2 + w^2) \\ I_z = \frac{1}{12}m(l^2 + h^2) \end{cases} \quad (2)$$

With  $m, l, w, h$  corresponding to TACO's mass when attached to the phantoms' arms, length, width and height, respectively. The moments of inertia of the PHANToM arms were not considered due to the complexity of the design of the PHANToM<sup>TM</sup> device. Digit peak forces and torques were extracted for and analyzed only for the first five perturbations in order to have an equal number of periodic and aperiodic perturbations. Linear mixed model (LMM; [1]) with repeated measure structure was used to analyze the data.

## 4 RESULTS

### 4.1 Center of pressure for individual participants

We first investigated the locations of the fingers on the TACO during the holding phase. By doing so, we aimed to investigate the digit CoP variability. Figure 4 shows CoP data for individual participants. We recorded a high variability between participants' digit location on the TACO (initial locations). In addition, the digit horizontal locations were not located all at the same line (Figure 4) as was the case in the previous studies using a manipulandum that constrained finger placement.

Table 1: Digit CoP results

Finger	$CoP_x : M \pm SE$ (cm)	$CoP_y : M \pm SE$
Thumb	$0.54 \pm 0.27$	$1.75 \pm 0.11$
Index	$-2.57 \pm 0.45$	$1.22 \pm 0.28$
Middle	$0.73 \pm 0.42$	$0.23 \pm 0.39$
Ring	$2.94 \pm 0.48$	$0.60 \pm 0.32$
Little	$5.23 \pm 0.44$	$1.57 \pm 0.19$

### 4.2 Grip force vs digit placements

Secondly, we aimed to evaluate the modulation of the grip force ( $F_{grip}$ ) within the range of modulation of horizontal and vertical locations ( $\Delta CoP_x$  and  $\Delta CoP_y$ , respectively) to investigate the effect of the above described digit contact modulation on  $F_{grip}$ . In this analysis, we averaged each participant data across five perturbations. LMM was used to fit  $F_{grip}$  data as a function of both  $\Delta CoP_x$  and  $\Delta CoP_y$  as follows:

$$y = X\beta + Zb + \epsilon \quad (3)$$

where  $y$  represents digits normal forces,  $X$  is model matrix for the vector of fixed effects  $\beta$ ,  $Z$  is the model matrix for the random effects vector  $b$ , and  $\epsilon$  is a residual vector for random effects. In the used model, we included  $\Delta CoP_x$  as a fixed effect and participants as random effect while allowing the adjustment to their  $CoP_s$ . We used the same LMM that was applied for both  $\Delta CoP_x$  and  $\Delta CoP_y$  (they were not included in the model at the same time).

Table 2 summarizes the different slopes and intercepts estimated by LMM for each participant. For horizontal displacements  $\Delta CoP_x$ , the estimated slope by LMM was largely different from zero for 4 participants (5 participants with negative slope and 2 participant with positive slope; Figure 5). For vertical displacements  $\Delta CoP_y$ , the estimated slope by LMM was different from zero for 6 participants (6 participants with negative slope and 1 participants with positive slope; Figure 5). Next, we estimated the LMM fitting coefficients for  $\Delta CoP_x$  and  $\Delta CoP_y$  within 95% of their highest probability density credible intervals using Markov Chain Monte Carlo (MCMC) method in order to evaluate their effect on the grip force  $F_{grip}$ . The latter test revealed an effect of both horizontal and vertical digit displacements on the grip force ( $\Delta CoP_x$ :  $p = 0.04$ ;  $\Delta CoP_y$ :  $p < 0.001$ ). Overall, these results show the existence of a trend between digit placements on the grasped object and the produced grip force. Note that participants varied in their digit initial placement during the grasping which lead to different grip forces.

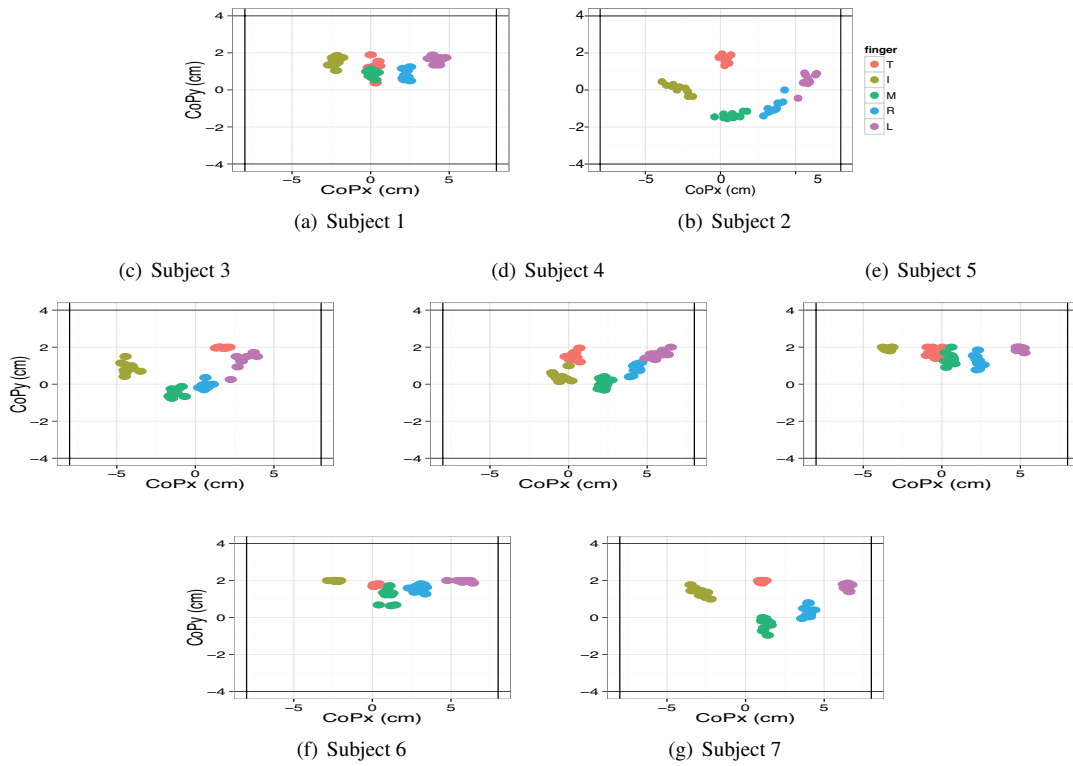


Figure 4: Digit CoP results for individual participants averaged across trials for each condition. The thumb CoPs were plotted at the same plane with other fingers (T: thumb, I: index, M: middle, R: ring, L: little).

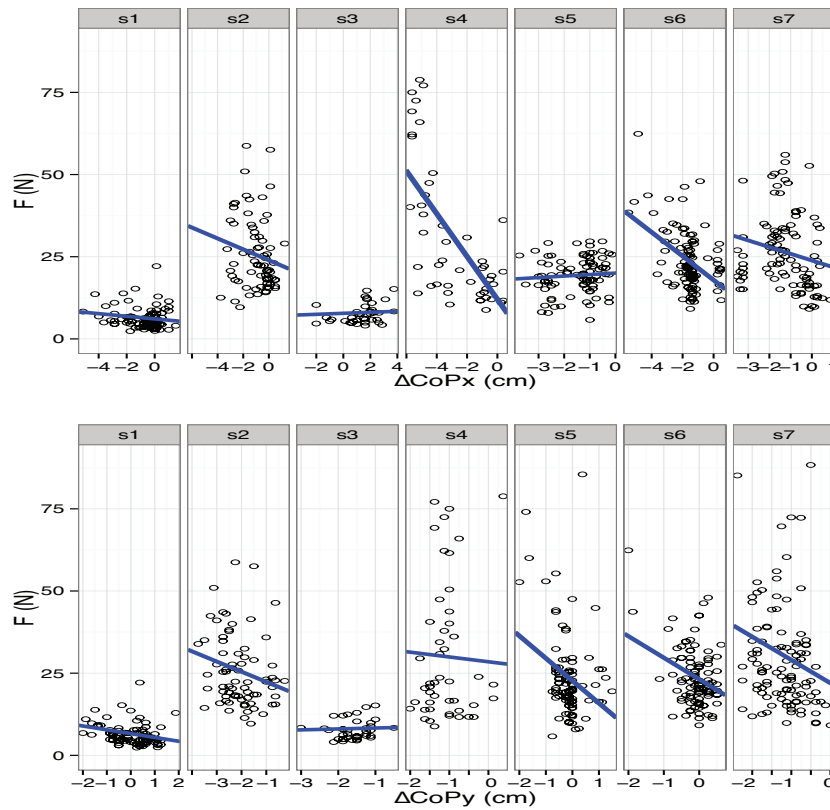


Figure 5: Grip force and  $\Delta CoP_{x,y}$  relationship for each participant. Lines represent the LMM fitting.

Table 2: LMM results for individual subjects:  $F_{grip} = a \cdot x + b$  ( $x: \Delta CoP_{x,y}$ )

	$a \cdot \Delta CoP_x + b$	$a \cdot \Delta CoP_y + b$
Subject 1	$-0.40 x + 6.09$	$-1.16 x + 6.60$
Subject 2	$-1.65 x + 23.92$	$-3.09 x + 23.70$
Subject 3	$0.15 x + 7.78$	$0.28 x + 8.59$
Subject 4	$-6.51 x + 12.03$	$-1.46 x + 28.04$
Subject 5	$0.45 x + 20.02$	$-6.82 x + 22.71$
Subject 6	$-3.64 x + 17.90$	$-6.54 x + 23.14$
Subject 7	$-2.04 x + 23.85$	$-7.06 x + 21.97$

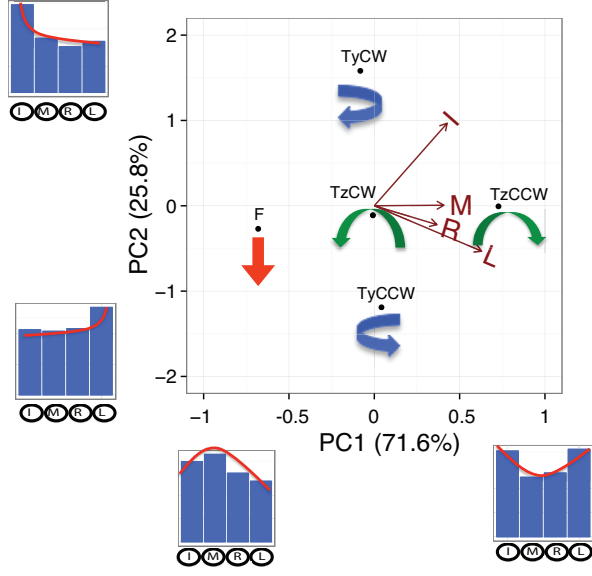


Figure 6: PCA results. Data points with blue and green arrows indicate PC loadings for all conditions. Brown vectors represent the PC loadings for each finger. The cosine angle between vectors indicates the correlation between the fingers. Blue bars represent digit normal forces.

### 4.3 Digit forces synergies

We investigated digit force synergies using principal component analysis (PCA). PCA was conducted on the mean peak forces, averaged across five perturbations and across participants for the fingers. The table for PCA analysis was constructed by defining digit forces as variables (columns) and conditions as the entries (rows). The results of the PCA revealed that the first two PCs accounted for 97% of the variance. Specifically, PC1 accounted for 71.6% of the variance while PC2 accounted for 25.8% of the variance. Figure 6 shows a biplot of the PCA for the index, middle, ring, and little fingers (I, M, R, L). Each finger force was characterized by 2 loadings,  $w_1$  and  $w_2$  ( $F_{finger} = w_1 PC1 + w_2 PC2$ ) that were represented by a vector (Figure 6). PC2 loadings were higher for the index and little fingers compared to the middle and ring (PC2 loading of middle finger was approximately zero). PC1 loadings were all positive for all fingers, while the PC2 loading was negative only for the index finger. The Figure 6 shows that the middle and ring fingers were more involved in supporting the load task within the conditions: perturbation  $F_y$ . The index finger was more involved in the rotational task within the conditions  $T_y^{CW}, T_z^{CCW}, T_z^{CW}$ . The little finger was more involved in the rotational tasks within the conditions  $T_y^{CCW}, T_y^{CW}, T_z^{CCW}$ . Finally, the cosine of the angle between arrows plotted in Figure 6 indicates the correlation between the fingers' forces.

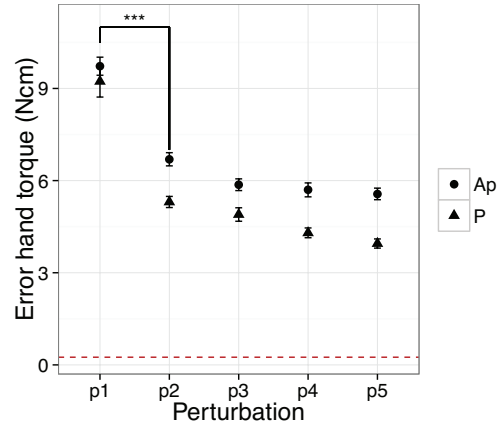


Figure 7: Hand compensatory torque error in the conditions periodic (P) and aperiodic (Ap) for the five perturbations.

### 4.4 Compensatory external torque

Finally, we explored trial-to-trial learning of digit position and force responses to compensate the external torque within the first five perturbations averaged across trials, participants, and perturbation type. This approach is justified by the fact that the perturbations were delivered in a consecutive fashion within a single trial. Figure 7 shows the error of hand compensatory torque for the periodic and aperiodic conditions for the five perturbations per trial. LMM was used to analyze the error of participants' hand torque using participants as random effects while the fixed effects were: perturbation frequency (periodic, aperiodic), perturbation number (p1, p2, p3, p4, p5), and number of trials. LMM revealed that the mean error in hand torque for the aperiodic condition was higher than the periodic one by ( $M \pm SE = 0.95 \pm 0.2$  N-cm). In addition, LMM revealed that the error in hand compensatory torque decreased by ( $M \pm SE = 0.001 \pm 0.003$  N-cm per trial). A posthoc analysis was conducted between two successive perturbations and revealed a significant effect between the first (p1) and second (p2) perturbations for both periodic and aperiodic conditions ( $p < 0.001$ ). Thus, participants learned to compensate the external torque within the earliest perturbation in each trial. Overall, these results indicate that the learning took place across perturbations and not across trials.

## 5 DISCUSSION

In this study we examined anticipatory control of digit forces and locations during unconstrained grasping tasks in response to force perturbations that were applied in a predictable or unpredictable fashion. An important feature of our experimental design was that subjects could choose digit placement across trials. The present results revealed that participants adopted different postures during grasping tasks as indicated by across-subject variability in digit  $CoP$ . In addition, digit force responses tended to vary systematically with digit horizontal and vertical spacing between the thumb and virtual finger. Moreover, results of PCA on digit forces revealed that two first PCs accounted for more than 95% of the variance.

The large between-subject variability in digit  $CoPs$  resulted from variability in both horizontal and vertical digit location ( $CoP_x$  and  $CoP_y$ ). This confirmed results found by [6] whom investigated unconstrained gripping using two-digit grasps. In [6], subjects adapted the vertical spacing between the thumb and index fingers before grasping in order to compensate the external torque whose direction was changed across blocks of consecutive trials. In contrast to previous studies that investigated multi-digit prehension could not assess modulation of digit contacts because they studied constrained grasping [15, 19]. This variability across subjects'

initial digit placements can be explained by idiosyncratic grasping strategies. It has been shown that subjects applied less grip forces when the grasping task was unconstrained [6], implying that digit normal forces were optimally controlled in terms of energy based on the actual digit locations. Moreover, we found that digit-force responses co-varied with the high variability recorded in horizontal and vertical digit locations  $CoP_{x,y}$ . Specifically, horizontal and vertical spacing between the thumb and the virtual finger altered the modulated grip force (Figure 5). Fu *et al.* [6] reported a significant correlation between the load force and vertical  $CoP_y$  (equivalent to  $CoP_x$  in our study). Thus, with the current results we submit that the modulation of the grip force is achieved based on actual digit location.

PCA revealed that middle and ring fingers are primarily involved in generating load task and that index and little fingers are primarily involved in rotational tasks. These results are consistent with what was found and named finger specialization in previous studies on multi-digit synergies [11, 17, 18] using a manipulandum with fixed digit locations. An important finding is that, despite the large variability in digit  $CoP_{x,y}$  and the existence of a trend between the digit normal forces and their locations, the proposed finger specialization still persists due to the external torque that was generated around the TACO's center of mass and the number of digits used. Moreover, the PCA analysis was conducted on digit forces averaged across participants, consequently, reducing between participants variability.

Participants accurately produced the compensatory torque within the first few perturbations in each trial. Furthermore, the learning effect was noticeable within a single trial and not across trials. In contrast, Fu *et al.* [6] reported that participants learned across trials. Recall, in [6] only one perturbation was induced during the lifting phase and it was induced during lifting the object (hence, its timing could be predicted). In contrast, in our study participants experienced several perturbations within the holding phase in each trial. The mechanical requirements for the grasping task during the lifting (dynamic) and holding (static) phase are different. Indeed, it has been shown that the grip force modulation tends to be different between the lift and holding phases [7, 10]. In addition, it has been shown that different categories of neuron populations fire during the dynamic and holding phase in monkeys [13, 12]. Mrotek *et al.* [10] suggested that the amount of the active tactile afferent, greater during the lifting phase than in the holding phase, facilitate the force responses modulation during the gripping task using thumb and index fingers.

Overall, participants learned to compensate sudden external torques after the first perturbation within each trial. Moreover, they varied in their initial digit placements leading to concurrent modulation in grip force. Thus, we conclude that the central nervous system coordinates multiple digits normal forces based on the proprioceptive feedback, self-chosen digit CoPs, and visual feedback of object orientation within and across trials. Therefore, the control of digit normal force is achieved in a way to compensate the redundancy in digit initial locations on the grasped object.

## ACKNOWLEDGMENT

We would like to thank authors of [16] for providing us the tactile modules. This work was partially supported by a Collaborative Research Grant BCS-1153034 (MS), by the European Commission under IP grant no. 248587 "THE Hand Embodied", by the European Commission under IP grant no. 601165 "WEARable HAPTics" and by the DFG Center of Excellence EXC 277: Cognitive Interaction Technology (CITEC).

## REFERENCES

[1] R. Baayen, D. Davidson, and D. Bates. Mixed-effects modeling with crossed random effects for subjects and items. *Journal of Memory and*

*Language*, 59(4):390–412, Nov. 2008.

[2] G. Baud-Bovy and J. F. Soechting. Two Virtual Fingers in the Control of the Tripod Grasp. *Journal of Neurophysiology*, 86:604–615, 2001.

[3] N. Bernstein. *The Co-ordination and Regulation of Movements*. Oxford, UK: Pergamon Press, 1967.

[4] J. Friedman and T. Flash. Task-dependent selection of grasp kinematics and stiffness in human object manipulation. *Cortex*, 43(3):444–460, Apr. 2007.

[5] Q. Fu, Z. Hasan, and M. Santello. Transfer of learned manipulation following changes in degrees of freedom. *Journal of Neuroscience*, 31(38):13576–13584, Sept. 2011.

[6] Q. Fu, W. Zhang, and M. Santello. Anticipatory planning and control of grasp positions and forces for dexterous two-digit manipulation. *Journal of Neuroscience*, 30(27):9117–9126, July 2010.

[7] R. S. Johansson and J. R. Flanagan. Coding and use of tactile signals from the fingertips in object manipulation tasks. *Nature Reviews Neuroscience*, 10(5):345–359, May 2009.

[8] R. S. Johansson and G. Westling. Roles of glabrous skin receptors and sensorimotor memory in automatic control of precision grip when lifting rougher or more slippery objects. *Experimental Brain Research*, 56(3):550–564, 1984.

[9] J. Lukos, C. Ansuini, and M. Santello. Choice of contact points during multidigit grasping: effect of predictability of object center of mass location. *Journal of Neuroscience*, 27(14):3894–3903, Apr. 2007.

[10] L. A. Mrotek, B. A. Hart, P. K. Schot, and L. Fennigkoh. Grip responses to object load perturbations are stimulus and phase sensitive. *Experimental Brain Research*, 155(4):413–20, Apr. 2004.

[11] J. Park, V. M. Zatsiorsky, and M. L. Latash. Optimality vs. variability: an example of multi-finger redundant tasks. *Experimental Brain Research*, 207(1-2):119–32, Nov. 2010.

[12] I. Salimi, T. Brochier, and A. M. Smith. Neuronal activity in somatosensory cortex of monkeys using a precision grip. i. receptive fields and discharge patterns. *Journal of Neurophysiology*, pages 825–834, 1999.

[13] I. Salimi, T. Brochier, and A. M. Smith. Neuronal activity in somatosensory cortex of monkeys using a precision grip. iii. responses to altered friction perturbations. *Journal of Neurophysiology*, 81:845–857, 1999.

[14] M. Santello, M. Flanders, and J. F. Soechting. Postural hand synergies for tool use. *Journal of Neuroscience*, 18(23):10105–10115, Dec. 1998.

[15] M. Santello and J. F. Soechting. Force synergies for multifingered grasping. *Experimental Brain Research*, 133(4):457–467, Aug. 2000.

[16] C. Schurmann, R. Koiva, R. Haschke, and H. Ritter. A modular high-speed tactile sensor for human manipulation research. In *World Haptics Conference (WHC), 2011 IEEE*, pages 339–344, June 2011.

[17] Y.-H. Wu, V. M. Zatsiorsky, and M. L. Latash. Multi-digit coordination during lifting a horizontally oriented object: synergies control with referent configurations. *Experimental Brain Research*, 222(3):277–90, Oct. 2012.

[18] V. M. Zatsiorsky, R. W. Gregory, and M. L. Latash. Force and torque production in static multifinger prehension: biomechanics and control. I. Biomechanics. *Biological Cybernetics*, 87(1):1–19, 2002.

[19] V. M. Zatsiorsky and M. L. Latash. Multi-finger Prehension: An overview. *Journal of Motor Behavior*, 40:446–476, 2008.